BISAR ALGORITHMS AND MATLAB IMPLEMENTATION

Andon D. Lazarov[1], Todor P. Kostadinov[2]

[1]Dept. of Informatics and Technical Sciences Burgas Free University Burgas, Bulgaria

[2]Institute of Information and Communication Technologies, Bulgarian Academy of Sciences Sofia, Bulgaria

Abstract: *This paper deals with program implementation of Bistatic Inverse Synthetic Aperture Radar (BISAR) using to extract a high resolution image of a moving target. BISAR is a bistatic topology with stationary transmitter and receiver and a moving target. The transmitter, receiver and target, represented as an assembly of point scatterers are situated in separate coordinate systems. Geometrical and kinematical equations and a mathematical model of deterministic LFM BISAR signal are described. A program code of signal formation and image extraction is implemented in MATLAB.*

Key words: *BISAR LFM model, BISAR algorithms and program implementation*

1. Introduction

BISAR is a system which transmitter and receiver are stationary situated and spatially separated. It is a remote sensing microwave method to monitoring targets and extracting their images. Bistatic concept in Inverse Synthetic Aperture Radar goals to enlarge the area of application and substantially improve the imaging radars functionality. The focus is on the program implementation of BISAR kinematical equations, signal mathematical formation and reconstruction procedure including motion compensation, range and azimuth compression by FFT.

BSAR concept in SAR for Earth observation and BSAR spaceborne performance are analyzed in [1, 2]. Several bistatic configurations on ISAR imaging have been proposed in [3, 4]. BSAR techniques for image reconstruction have been investigated in [5-7]

In this work geometry of BISAR scenario including spatially separated transmitter and receiver, and a target described in a separate coordinate system is considered. BISAR is based on the relative target movement with respect to the stationary transmitter and receiver. The separation of transmitter and receiver (the bistatic geometry) provides further enhancement of the microwave remote sensing and imaging systems. The returned signal is formed by an assembly of linear frequency modulated pulses emitted from the transmitter, reflected by the target object and returned in the receiver. It is demodulated by complex conjugated emitted waveform multiplication. The image function can be extracted from two dimensional signal using an inverse operation and in order to improve the image quality a motion compensation procedure has been applied.

Main purpose of this work is the program realization and implementation in Matlab environment of the process of BISAR LFM signal formation. The signal is reflected by a marine target.

The paper is organized as follows: In Section 2 BISAR geometry and kinematical equations are presented. In Section 3 mathematical BISAR LFM signal model and image reconstruction procedure are given. In Section 4 program implementation of BISAR algorithm is described. In Section 5 numerical experiment is carried out. In Section 6, conclusions about BISAR algorithms effectiveness is drawn.

2. BISAR geometry and kinematics

The three dimensional BISAR scenario illustrated in Fig. 1 includes stationary transmitter described by the position vector $\mathbf{R}^s$, receiver described by $\mathbf{R}^r$ and a marine target all situated in Cartesian coordinate system *Oxyz*. $\mathbf{R}^s(p)$ and $\mathbf{R}_{00'}(p)$ are the current position vectors of the transmitter in discrete time instant p and of the mass centre of the target. The target is presented as an assembly of point scatterers in Cartesian coordinate system OXYZ, where $\mathbf{R}_{ijk}$ is the position vector of *ijk*th point scatterer.

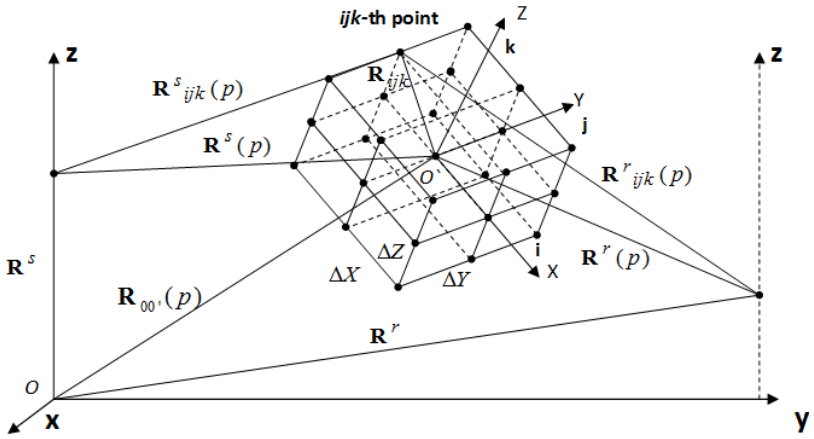

Figure 1. BISAR geometry

The position vector from the transmitter to the object mass centre $\mathbf{R}^s_{0'}(p)$ is defined by:

$$\mathbf{R}^s(p) = \mathbf{R}^s - \mathbf{R}_{00'}(p) = \mathbf{R}^s - \mathbf{R}_{00'}(0) - \mathbf{V}\left(\frac{N}{2} - p\right)T_p, \tag{2}$$

where $\boldsymbol{V}$ is the target vector velocity, $p = \overline{1,N}$ is the number of the current emitted pulse, $\boldsymbol{N}$ is the number of pulses and T_p is the pulse repetition period.

Range vector-distance from the target mass centre to the receiver

$$\mathbf{R}^r(p) = \mathbf{R}^r - \mathbf{R}_{00'}(p) = \mathbf{R}^r - R_{00'}(0) - \mathbf{V}\left(\frac{N}{2} - p\right)T_p \tag{3}$$

Range vector-distance from the transmitter to the *ijk*th point scatterer

$$\mathbf{R}^s{}_{ijk}(p) = \mathbf{R}^s(p) + \mathbf{A}\mathbf{R}_{ijk} = \mathbf{R}^s - \mathbf{R}_{00'}(0) - \mathbf{V}\left(\frac{N}{2} - p\right)T_p + \mathbf{A}\mathbf{R}_{ijk} \tag{4}$$

Range vector-distance form the *ijk*th point scatterer to the receiver

$$\mathbf{R}^r{}_{ijk}(p) = \mathbf{R}^r(p) - \mathbf{A}\mathbf{R}_{ijk} = \mathbf{R}^r - \mathbf{R}_{00}(0) - \mathbf{V}\left(\frac{N}{2} - p\right)T_p - \mathbf{A}\mathbf{R}_{ijk} \tag{5}$$

The round trip distance transmitter-*ijk*th point scatterer-receiver can be expressed as

$$R_{ijk}(p) = \frac{\left|\mathbf{R}^s{}_{ijk}(p)\right| + \left|\mathbf{R}^r{}_{ijk}(p)\right|}{2} \tag{6}$$

3. LFM BISAR signal model

BISAR signal is composed of series of linear frequency modulated pulses emitted from the transmitter towards the object, each of which is described by

$$\dot{S}(t) = \mathbf{rect}\frac{t}{T}\mathbf{exp}\left\{-j\left[\omega t + bt^2\right]\right\} \tag{7}$$

where $\omega = 2\pi\frac{c}{\lambda}$ is the angular frequency; $c = 3.10^8$ m/s is the speed of the light; λ is the wavelength of the signal; T is the time duration of the LFM pulse; $b = \frac{2\pi\Delta F}{T}$ is the LFM rate.

The deterministic component BISAR signal, returned by the *ijk*th point scatterer has following expression:

$$\dot{S}_{ijk}(p,t) = a_{ijk}\mathbf{rect}\frac{t - t_{ijk}(p)}{T}\mathbf{exp}\left\{-j\left[\omega\left(t - t_{ijk}(p)\right) + b\left(t - t_{ijk}(p)\right)^2\right]\right\}, \tag{8}$$

where

$\mathbf{rect}\frac{t - t_{ijk}(p)}{T} = \begin{cases} 1, 0 \le \frac{t - t_{ijk}(p}{T} < 1, \\ 0, \text{otherwise.} \end{cases}$ is a rectangular filtering function for the returned signal, a_{ijk} is the reflection coefficient of the ijk th point scatterer, a three-dimensional (3-D) image function; $t_{ijk}(p) = \frac{R_{ijk}(p)}{c}$ is the round trip time delay of the ijk th point scatterer signal. BISAR signal deterministic component can be expressed as a superposition of signals reflected form all target point scatterers:

$$\dot{S}(p,t) = \sum_{ijk} a_{ijk}\mathbf{rect}\frac{t - t_{ijk}(p)}{T}\mathbf{exp}\left\{-j\left[\omega\left(t - t_{ijk}(p)\right) + b\left(t - t_{ijk}(p)\right)^2\right]\right\}. \tag{9}$$

BISAR returned signal demodulation is a multiplication procedure of a complex conjugated emitted LFM waveform:

$$\hat{S}(p,k) = \sum_{ijk} a_{ijk}\mathbf{rect}\frac{t_{ijk\,\min}(p) + (k-1)\Delta T - t_{ijk}(p)}{T}\mathbf{exp}\left[-j\begin{pmatrix}\omega(t_{ijk\,\min}(p) + (k-1)\Delta T - t_{ijk}(p)) - \\ -b\left((t_{ijk\,\min}(p) + (k-1)\Delta T - t_{ijk}(p)\right)^2\end{pmatrix}\right] \tag{10}$$

which is a space transformation of 3-D image function to 2-D BISAR signal plane.

4. Image reconstruction algorithm

The image function $a_{ijk}(\hat{p},\hat{k})$ can be extracted from 2-D BISAR signal plane by the inverse projective operation

$$a_{ijk}(\hat{p},\hat{k}) = \sum_{p=1}^{N}\sum_{k=1}^{K}\hat{S}(p,k).\exp\left[j\begin{pmatrix}\omega(t_{ijk\,\min}(p) + (k-1)\Delta T - t_{ijk}(p)) - \\ -b\left((t_{ijk\,\min}(p) + (k-1)\Delta T - t_{ijk}(p)\right)^2\end{pmatrix}\right] \tag{11}$$

where $\hat{p}$ and $\hat{k}$ are the range and azimuth discrete coordinates of the *ijk*th point scatterer.

The substitution of the exponential term in expression (11) by Taylor expansion yields

$$a_{ijk}(\hat{p},\hat{k}) = \sum_{p=1}^{N}\left[\sum_{k=1}^{K}\hat{S}(p,k).\exp\left[j\Phi(p,k)\right]\exp\left(j2\pi\frac{k\hat{k}}{K}\right)\right]\exp\left(j2\pi\frac{p\hat{p}}{N}\right). \qquad (12)$$

where $\Phi(p,k) = a_2.(pT_p)^2 + ... + a_m(pT_p)^m + b_2.(k\Delta T)^2 + ... + b_m(k\Delta T)^m$ is the phase correction term of higher order, a_m and b_m are the coefficients of the polynomial of higher order.

The image reconstruction procedure includes the following stages:

Phase correction: $\widetilde{S}(p,k) = \hat{S}(p,k).\exp\left[j\Phi(p,k)\right]$;

Range compression: $\widetilde{S}(p,\hat{k}) = \frac{1}{K}\sum_{k=1}^{K}\widetilde{S}(p,k).\exp\left(j2\pi\frac{k\hat{k}}{K}\right)$;

Azimuth compression: $a_{ijk}(\bar{p},\bar{k}) = \frac{1}{N}\sum_{p=1}^{N}\widetilde{S}(p,\bar{k}).\exp\left(j2\pi\frac{p\hat{p}}{N}\right)$,

where range and azimuth (cross range) compression are accomplished by two discrete Fourier transforms

5. Program implementation of BISAR algorithms

As a high level program language Matlab is a convenient tool for signal processing and mathematical analysis. The variety of built in operators makes it ideal for description of aperture synthesis, geometrical and mathematical apparatus of BISAR geometry and detailed graphical representation of the results.

Every program segment begins with reservation of memory and closure of all previous opened figures. After that there will be sufficient operational memory and data file, containing real data, or previously computed results including vector-coordinates can be loaded. The variables needed in the process of modeling are also defined as follow:

```
load battle_ship.mat
num=max(size(xyz));
xrs=-250; yrs=0; zrs=15; xrr=300; yrr=0; zrr=12;
x0=100; y0=100; z0=0; x00=25; y00=50; z00=0;
N=256; K=256; f=10^10; Tp=0.0032; T=10^-6; deltaF=2*10^8;
omega=2*pi*f; c=3*10^8;
b=2*pi*deltaF/T; deltaT=T/K; a=0.5
```

The program segment that describes the orientation of the plane, in which the target is situated, can be written as:

```
alpha=pi/2; beta=pi; gama=pi/2; galpha=pi;
V=14; Vx= V*cos(alpha); Vy=V*cos(beta); Vz= V*cos(gama);
A0=Vz*(y00-y0)-Vy*(z00-z0); B0=Vx*(z00-z0)-Vz*(x00-x0);
C0=Vy*(x00-x0)-Vx*(y00-y0); D=(A0)^2+(B0)^2+(C0)^2;
Ag=(A0*V*cot(galpha)+C0*Vy-B0*Vz)/D;
Bg=(B0*V*cot(galpha)+A0*Vz-C0*Vx)/D;
Cg=(C0*V*cot(galpha)+B0*Vx-A0*Vy)/D;
D1=(Ag)^2+(Bg)^2+(Cg)^2; psi=atan(-Ag/Bg);
theta=acos(Cg/sqrt(D1));
phi=acos((Vx*Bg-
Vy*Ag)*sqrt(((Ag)^2+(Bg)^2)*((Vx)^2+(Vy)^2)+(Vz)^2));
a11=cos(psi)*cos(phi)-sin(psi)*cos(theta)*sin(phi);
a12=-cos(psi)*sin(phi)-sin(psi)*cos(theta)*cos(phi);
a13=sin(psi)*sin(theta);
a21=sin(phi)*cos(phi)+cos(psi)*cos(theta)*sin(phi);
a22=-sin(psi)*sin(phi)+cos(psi)*cos(theta)*cos(phi);
a23=-cos(psi)*sin(theta); a31=sin(theta)*sin(phi);
a32=sin(theta)*cos(phi);a33=cos(theta);
A_rot=[a11 a12 a13; a21 a22 a23; a31 a32 a33];
transf_xyz=delta.*A_rot*xyz;
```

The *ijk*th point distance vector from the object space and its corresponding time delay are calculated by applying a Kronecker tensor operator to the object's-coordinates. In order to define the vector-coordinates of the point scatterers along with the vector displacement, matrix multiplication is applied.

```
p_v=(0:N-1);
Xs=kron(x00,ones(num,N))-kron(xrs,ones(num,N))+kron(Vx*(N/2-
p_v)*Tp,ones(num,1))+kron(transf_xyz(1,:),ones(N,1)).';
Ys=kron(y00,ones(num,N))-kron(yrs,ones(num,N))+kron(Vy*(N/2-
p_v)*Tp,ones(num,1))+kron(transf_xyz(2,:),ones(N,1)).';
Zs=kron(z00,ones(num,N))-kron(zrs,ones(num,N))+kron(Vz*(N/2-
p_v)*Tp,ones(num,1))+kron(transf_xyz(3,:),ones(N,1)).';
Xr=kron(xrr,ones(num,N))-kron(x00,ones(num,N))+kron(Vx*(N/2-
p_v)*Tp,ones(num,1))+kron(transf_xyz(1,:),ones(N,1)).';
Yr=kron(yrr,ones(num,N))-kron(y00,ones(num,N))+kron(Vy*(N/2-
p_v)*Tp,ones(num,1))+kron(transf_xyz(2,:),ones(N,1)).';
Zr=kron(zrr,ones(num,N))-kron(z00,ones(num,N))+kron(Vz*(N/2-
p_v)*Tp,ones(num,1))+kron(transf_xyz(3,:),ones(N,1)).';
Rs=sqrt((Xs).^2+(Ys).^2+(Zs).^2);
Rr=sqrt((Xr).^2+(Yr).^2+(Zr).^2);
t=(Rs+Rr)./c;
```

By preliminary definition of arrays, computational performance and optimal memory usage are obtained:

```
E1=zeros; func=zeros; rect=zeros;
S1=zeros; Se=zeros; S=zeros(N,K,1);
S2=zeros(N,K,1);
```

The calculation of deterministic LFM BISAR signal is a cyclic one with respect to discrete range and azimuth coordinates. Iteratively a rectangular function for each range and cross-range

coordinates is calculated in order to select signals taking part in signal formation the BISAR signal phase value of selecting rectangular function and the complex amplitude of the LFM signal are computed. Recurrent sum along the discrete coordinates and demodulation is performed:

```
for q=1:num

    for p=1:N
        for k=1:K
            E1(p,k,q)=min(t(:,p))+(k-1)*deltaT-t(q,p);
            func(p,k,q)=E1(p,k,q)/T;
            if func(p,k,q)>=0&&func(p,k,q)<1
                rect(p,k,q)=1;
            else
                rect(p,k,q)=0;
            end
S1(p,k,q)=rect(p,k,q)*exp(1j*(omega*E1(p,k,q)+b*E1(p,k,q)^2));
Se(p,k,q)=exp(-1j*(omega*(k-1)*deltaT+b*((k-1)*deltaT)^2));
S(p,k,1)=S(p,k,1)+S1(p,k,q)*Se;
        end
    end
end
```

Autofocusing phase compensation is implemented by consecutively increase of a phase correction coefficient a_2 from the polynomial as illustrated by the following program segment:

```
a21=0; delta2=0.5*10^0;
for a2=1:10000
a21=a21+delta2; F2=exp(1j.*(a21.*((1:128).*Tp).^2));
            for k = 1:128;
                Sdem_F2(:,k) = S(:,k) .*F2;
            end
fft12=abs(fftshift(fft(transpose(fft(Sdem_F2)))));
            Sfoc2=fft12./max(max(fft12));
            for k_f=1:N
average2(:,k_f)=(Sfoc2(:,k_f).^2)/sum(sum(Sfoc2.^2));
Entropylog2(:,k_f)=average2(:,k_f).*log(average2(:,k_f));
            end
            Entropy2(a2) = -sum(sum(Entropylog2));
            if a2>1
                  dif_entropy2(a2)=diff([Entropy2(a2-1);
            else
                dif_entropy2(a2)=NaN;
            end
    end
```

Range and azimuth compression are implemented by Fast Fourier Transform in discrete range and azimuth coordinates, spectrum shift and estimation of the amplitude value of the returned signal:

```
A1=fft(S); A2=fft(transpose(A1));
A3=fftshift(A2); absolute=abs(A3);
```

The aforementioned BISAR algorithms and their Matlab description are used in implementation of numerical experiments. Matlab realization of the algorithms is also used to validate the BISAR signal formation and reconstruction procedures.

6. Numerical experiment

In order to verify BISAR geometry, signal formation and image reconstruction, numerical experiment is carried out. It is assumed that the target is moving rectilinearly in Cartesian coordinate system *Oxyz*. The transmitter coordinates are $x^s = -45$ m; $y^s = 0$ m; $z^s = 25$ m. Coordinates of the receiver: $x^r = 38$ m; $y^r = 0$ m; $z^r = 10$ m. target parameters are: module of the vector velocity $V = 14$ m/s; $\alpha = \pi/2$; $\beta = -\pi$; $\gamma = \pi/2$. The coordinates of the mass-center at the moment $p = N/2$: $x_{00}(0) = 25$ m; $y_{00}(0) = (50)$ m; $z_{00}(0) = 0$ m.

BISAR LFM signal parameters are: wavelength $\lambda = 3.10^{-2}$ m, pulse repetition period $T_p = 10^{-3}$ s, LFM pulsewidth $T = 10^{-6}$ s, number of samples of LFM transmitted signal $K = 256$, carrier frequency $f = 10^{10}$ Hz., LFM sampling period $\Delta T = T/K = 3.9.10^{-9}$ s, LFM signal bandwidth $\Delta F = 2.10^8$ Hz, LFM rate $b = 1{,}39.10^{14}$, number of transmitted pulses $N = 256$. The 3-D regular grid where the target object is located has cell dimensions $\Delta X = \Delta Y = \Delta Z = 0.5$ m. BISAR signal, BISAR range compressed signal and BISAR azimuth compressed signal for $x_{00}(0) = 0$ m.; $y_{00}(0) = 20$ m.; $z_{00}(0) = 0$ m. are depicted in Figures 2, 3 and 4. Unfocused reconstructed image is shown in Fig. 5.

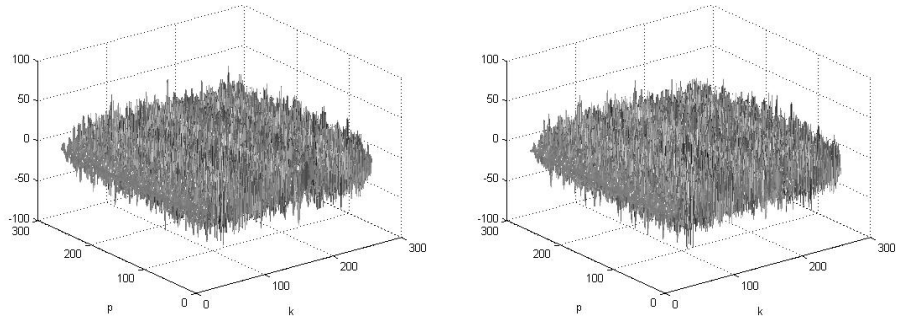

Figure 2. BISAR signal: real (a) and (b) imaginary part.

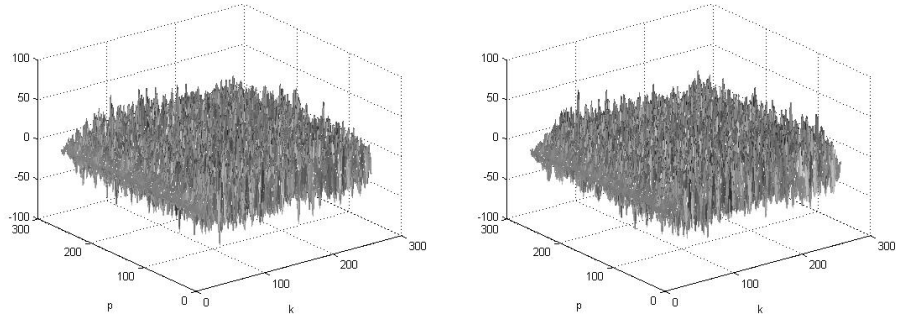

Figure 3. Demodulated BISAR signal: real (a) and (b) imaginary part.

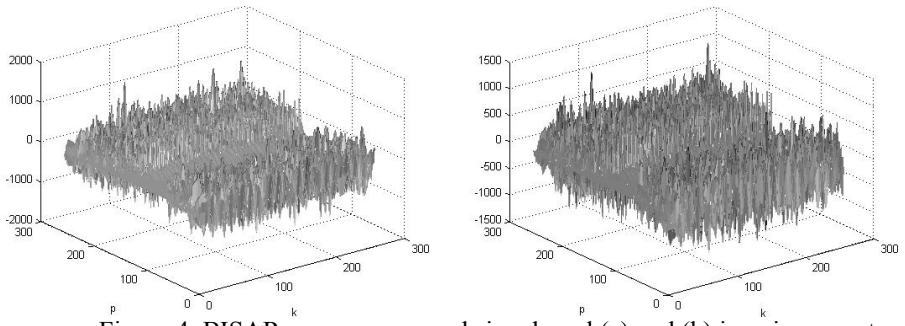

Figure 4. BISAR range compresed signal: real (a) and (b) imaginary part.

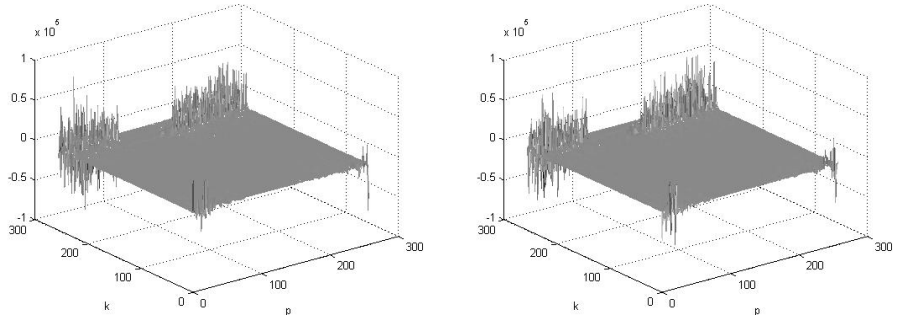

Figure 5. BISAR azimuth compressed signal: real (a) and (b) imaginary part.

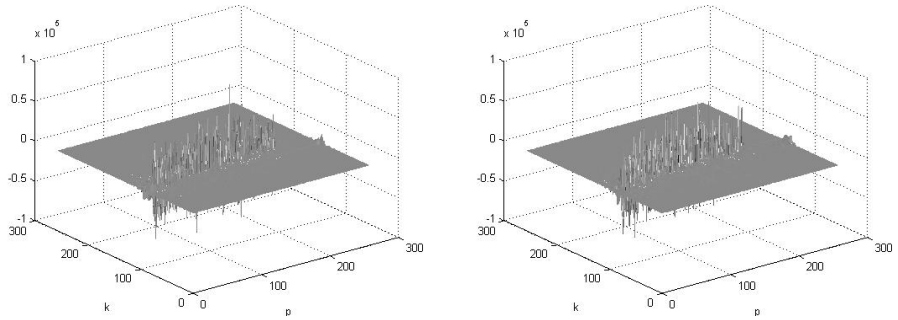

Figure 6. BISAR azimuth compressed and shifted signal: real (a) and (b) imaginary part.

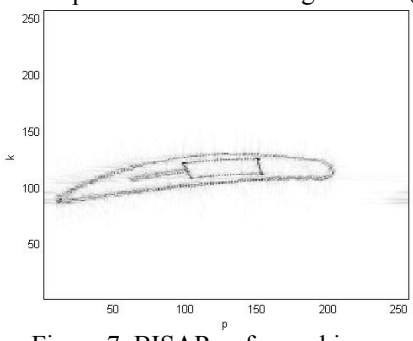

Figure 7. BISAR unfocused image.

In Figures 8 - 10 BISAR signal models and results of the reconstruction of a target's focused image are depicted. The focusing function is approximated only by its quadratic component.

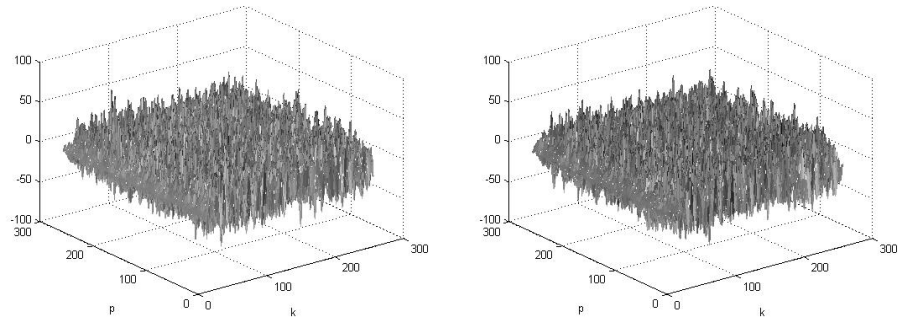

Figure 8. BISAR focused signal: real (a) and (b) imaginary part.

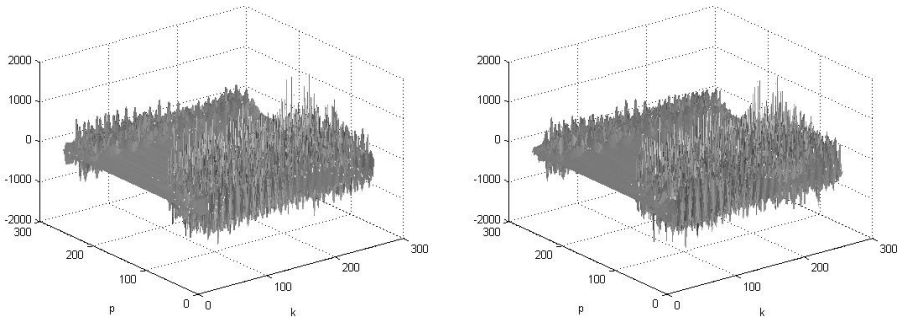

Figure 9. BISAR focused range compresed signal: real (a) and (b) imaginary part.

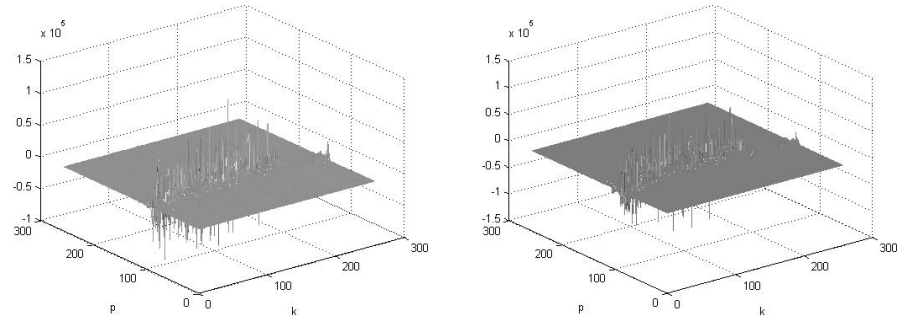

Figure 10. BISAR focused azimuth compressed and shifted signal: real (a) and (b) imaginary part.

In Fig. 11 the evolution of the entropy function against the coefficient a_2 is depicted. The minimum value of the entropy function in the diapason of variation of coefficient a_2 from 0 to 671 with step $\Delta = 0.5$ is $H_s = 0.347$ and respectively the focused image is depicted in Fig. 12.

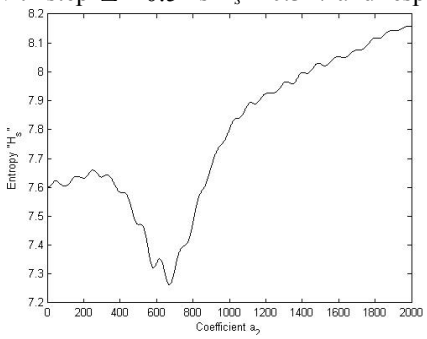

Figure 11. Entropy function evaluation for coeff. a_2

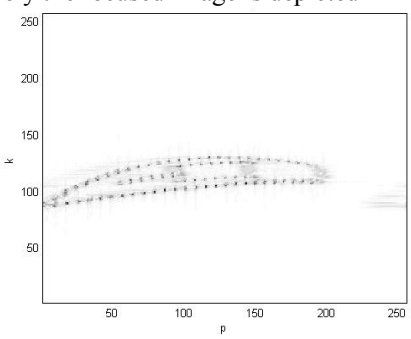

Figure 12. BISAR focused image.

7. Conclusion.

In the present work BISAR concept is considered. BISAR topology with stationary transmitter and receiver, and moving target has been specified. Kinematic vector equations have been derived. BISAR returned signal has been modeled. Image reconstruction by range compression and azimuth compression both implemented by Fourier transforms and phase compensation are defined. Geometrical and kinematical modeling, ISAR signal formation and phase correction based on BISAR concept have been implemented in Matlab environment. Numerical experiment confirms the correctness of BISAR signal model and autofocusing procedure, and their program realization.

Acknowledgment: This work is supported by Project - Support of PhD students, post doctors and young scientists in the area of computer science: BG 051PO001-3.3.04/13 and NATO CLG: ESP.EAP.CLG.983876

References:

[1] A. Moccia, Rufmo, G., D'Errico, M., Alberti, G., et. al. "BISSAT: A bistatic SAR for Earth observation", *Proc. of IEEE International Geoscience and Remote Sensing Symposium (IGARSS'02)*, Vol. 5, June 24-28, 2002, pp. 2628-2630.

[2] Moccia, A., Salzillo, G., D'Errico, M., Rufino, G., Alberti, G., "Performace of bistatic synthetic aperture radar", IEEE TRANSACTIONS ON AEROSPACE AND ELECTRONIC SYSTEMS VOL. 41, NO. 4 OCTOBER 2005, pp. 1383 – 1395

[3] Lazarov, A., Kabakchiev, C., Gashinova, M., Kostadinov, T., Ultra wide band bistatic forward scattering inverse synthetic aperture radar imaging, International Radar Symposium, Leipzig, Germany 7-9 September 2011 – to be published

[4] Lazarov, A., Kabakchiev, C., Rohling, H., Kostadinov, T., Bistatic Generalized ISAR concept with GPS waveform, International Radar Symposium, Leipzig, Germany 7-9 September 2011 – to be published

[5] O. Loffeld, Nies, H., Peters, V., and S. Knedlik,"Models and useful relations for bistatic SAR processing", *Proceedings of International Geoscience and Remote Sensing Symposium (IGARSS)*, vol. 3, Toulouse, France, July 21—25, 2003, pp. 1442—1445.

[6] J. H. G. Ender, I. Walterscheid, and A. R. Brenner,"New aspects of bistatic SAR: Processing and experiments."*2004 Proceedings of International Geoscience and Remote Sensing Symposium (IGARSS)*, vol. 3, Anchorage, AK, Sept. 20—24, 2004, pp. 1758—1762.

[7] D. D'Aria, A. M. Guarnieri, and F. Rocca, "Focusing bistatic synthetic aperture radar using dip move out", IEEE Transactions on Geoscience and Remote Sensing, 42, no. 7, 2004, pp. 1362—1376.